Thermal modification of magnetism in cobalt-doped ZnO nanowires grown at low temperatures

Jingbiao Cui and Ursula Gibson
Thayer School of Engineering, Dartmouth College, Hanover, New Hampshire 03755-8000 USA
(Received 14 February 2006; revised manuscript received 5 May 2006; published 17 July 2006)

The optical and magnetic stability of hydrothermally grown Co-doped ZnO nanowires were investigated. The experimental results suggest that two different kinds of coordination of Co ions in the ZnO host, either with or without magnetic coupling, likely coexist in the as-grown samples. Low-temperature annealing resulted in the transformation of the isolated ions to magnetically coupled ones, leading to the enhancement of ferromagnetic properties. High-temperature annealing (900 °C) leads to paramagnetic behavior and improved crystallinity of the ZnO host materials due to Co migration and the formation of nonmagnetic oxide clusters, as evidenced by photoluminescence, Raman scattering, x-ray diffraction, and electron microscopy.

DOI: 10.1103/PhysRevB.74.045416 PACS number(s): 75.50.Pp, 75.75.+a, 81.05.Dz

I. INTRODUCTION

Semiconductor materials doped with a few percent of transition metal [dilute magnetic semiconductors (DMSs)] can exhibit ferromagnetic properties and have potential applications in spintronic devices, which take advantage of both electron charge and spin in device operation.[1] Since the prediction of room temperature ferromagnetism in transition metal doped III-V and II-VI semiconductors by Deitl *et al.*[2] and Sato and Katayama-Yoshida,[3] great efforts have been made to synthesize and characterize DMS thin films and nanostructures. Among various host materials such as group IV elements, III-V semiconductors, and II-VI compounds, ZnO has been considered as one of the promising candidates for fabricating DMSs due to its high solubility for transition metals and superior semiconductor properties. ZnO is a wide band-gap semiconductor with a large exciton binding energy and has potential applications in electronic and optoelectronic devices.[4] ZnO thin films and nanostructures doped with a number of transition metals (Ni, Co, Fe, Cu, and Mn) have been experimentally demonstrated to exhibit ferromagnetism above room temperature.[5–13]

Various growth techniques including solid state reaction,[6,7] pulsed laser deposition,[5,8] reactive sputtering,[10] and vapor phase deposition[13] have been employed to deposit transition metal doped ZnO thin films at high temperatures ranging from 400 to 800 °C. In addition, room temperature ferromagnetism in Co-implanted ZnO samples followed by annealing at 700 °C was reported.[14] Recently, transition-metal-doped ZnO nanostructures were also investigated by several groups. For example, Co-doped ZnO nanowires with room temperature ferromagnetism were deposited by pulsed laser deposition at 400 °C (Ref. 13) and Mn-doped ZnO nanowires with magnetic ordering at −236 °C were grown using a vapor phase growth at 500 °C.[11] Cui and Gibson have used an electrochemical process at 90 °C to grow Co and Ni doped ZnO nanowire arrays and found ferromagnetism in the as-grown sample at 25 °C.[12] These advancements in the development of DMS nanostructures allow the exploration of new applications and underlying physics based on the special combination of quasi-one-dimensional structures and ferromagnetism in semiconductors.

Since the DMSs contain a few percent of transition metal impurities, thermal stability of the impurities and induced defects, which determine the material physical properties, are very important in terms of both practical applications and fundamental physical understanding. A few reports on the effects of annealing on magnetic properties of doped ZnO have been published recently with contradictory experimental results.[15–17] All the investigations indicated that the magnetization of the doped thin films or bulk materials was unstable at temperatures higher than the sample preparation temperature, i.e., between 500 and 700 °C. Thermal stability becomes a prominent issue for low-temperature-grown ZnO nanowires, in which impurities and defects are potentially less stable than those grown at high temperatures.

In this paper, we investigated the properties of low-temperature-grown Co-doped ZnO nanowires, thermally annealed at temperatures up to 900 °C. We use a combination of structural and optical analysis to determine the origins of the magnetic behavior. The Co-doped ZnO nanowire samples were grown by electrodeposition at 90 °C in an aqueous solution. It was found that annealing at temperatures lower than 400 °C significantly enhanced the magnetic properties of the doped nanowires, which we attribute to the transformation of nonmagnetic isolated Co^{2+} ions, as evidenced by photoluminescence, to *d*-band coupled ferromagnetic material. Continued annealing at higher temperatures caused the ferromagnetism to decrease and finally disappear at 900 °C. The change from ferromagnetism to paramagnetism may be explained by long-range migration of cobalt and the precipitation of Co oxides, based on x-ray diffraction and transmission electron microscopy evidence.

II. EXPERIMENTAL DETAILS

The Co-doped ZnO nanowire arrays were deposited in aqueous solution by an electrochemical assisted hydrothermal process. Zn nitrate hexahydrate $[Zn(NO_3)_2 \cdot 6H_2O]$ and hexamethylenetetramine $(C_6H_{12}N_4)$ were used as precursors for ZnO nanowire growth and Co nitrate hexahydrate $[Co(NO_3)_2 \cdot 6H_2O]$ was used as a source material for doping. The reagents were used as received from Alfa Aesar without further purification. Zinc nitrate hexahydrate (2.5 mmol), hexamethylenetetramine (2.5 mmol) and cobalt nitrate hexahydrate (in the amounts shown in Table I) were dissolved in 200 ml deionized water at room temperature and

TABLE I. Growth conditions for the samples used in this study.

Sample	Co nitrate (mmole)	Co in sample (%)	Growth time (h)
S0	0	0	1.5
S1	0.0125	0.48	1.5
S2	0.05	0.95	1.0
S3	0.125	2.3	1.0
S4	0.285	4.7	1.0
S5A	0.12	2.2	1.0
S5B	0.085	1.7	1.5

then heated to 90 °C on a hot plate in a covered container. A negative dc potential of −0.7 V relative to a 0.2 mm gold counter electrode was applied to a silicon substrate during the nanowire growth. N-type silicon wafers with (100) surface and a resistivity of 4–7 Ω cm were used. At the end of the growth period (1–1.5 h), the sample was removed from the solution and immediately rinsed in flowing deionized water to remove any residual salt from the surface. Samples were grown under similar conditions to verify the reproducibility of the observations.

The samples were characterized by scanning electron microscopy (SEM) (FEI XL-30 at 15 kV) equipped with an energy dispersive x-ray spectroscopy (EDX), transmission electron microscopy (TEM) (FEI Technon), x-ray diffraction (XRD) (Siemens diffractometer D5000, with Cu-Kα radiation, $\lambda = 1.5418$ Å), vibrating sample magnetometry (VSM) (Lakeshore), photoluminescence (PL), and a confocal Raman microscope (Witec, CRM 200). The nanowires were mechanically removed from the substrate and redeposited onto Cu grids for TEM measurement. Photoluminescence was measured at room temperature using a KrF (248 nm) excimer laser at an average intensity of 1 mW/mm^2. The laser pulse has width of 30 ns and repetition rate of 80 Hz. The emitted light was collected by a lens and transferred to an Ocean Optics detector via an optical fiber. The Raman spectrum was excited at 514 nm by an Ar ion laser and measured in a backscattering mode. Differential thermal analysis (DTA) curves were obtained with a Perkin Elmer DTA System 1700 using Al_2O_3 as the reference material. The samples were heated (25 °C/min) under flowing argon.

Annealing of both doped and undoped samples was performed in a quartz tube with flowing argon gas, holding the nanowires samples at the nominal temperature for 20 min unless otherwise stated. The samples were removed for characterization after cooling down for 15 min in the quartz tube. Subsequent annealing steps were performed on the samples at higher temperatures.

III. RESULTS AND DISCUSSION

A typical SEM image of pure ZnO nanowires (sample S0) is shown in Fig. 1(a). The nanowires are vertically aligned on the substrate and have diameters ~100–200 nm and lengths up to 2 μm. Figure 1(b) shows the SEM image of Co-doped ZnO nanowires (sample S3) grown under conditions similar to those used for the pure ZnO nanowire arrays. The composition of the pure and Co-doped ZnO nanowires was measured by EDX and shown in Fig. 1(c). In addition to an oxygen peak at 0.53 keV and Zn signals at 1.01, 8.63, and 9.58 keV, a cobalt peak at 6.94 keV was observed for the Co-doped ZnO nanowires. XRD analysis showed a change in the lattice constant after doping with Co, suggesting the incorporation of Co into ZnO crystalline structure.[5,12]

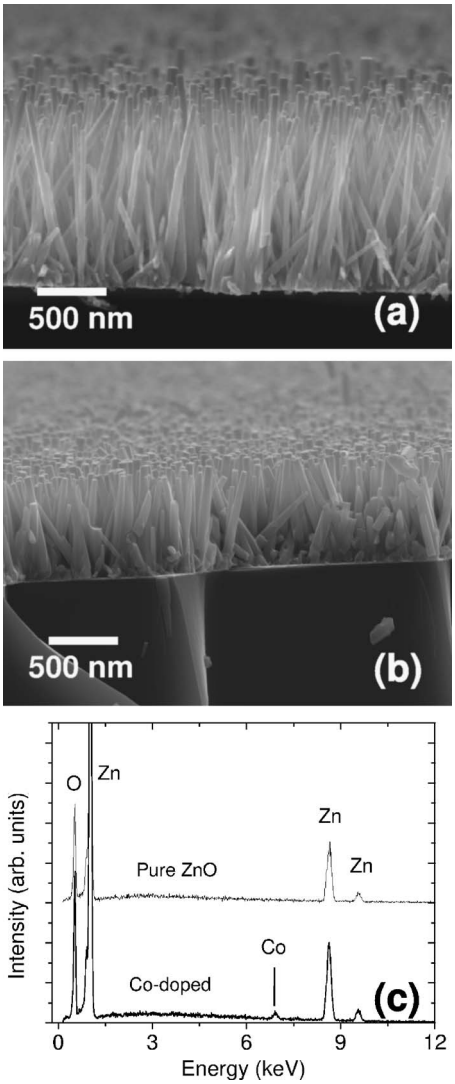

FIG. 1. SEM images of pure (a) and Co-doped ZnO nanowires arrays (b) deposited by an electrochemically assisted hydrothermal process at 90 °C. (c) EDX spectra taken on both pure and Co-doped ZnO nanowires.

A. Annealing effects on optical properties

Figure 2 displays the room temperature photoluminescence spectra taken on ZnO nanowires doped with Co at different concentrations (sample S0-S4). Note that the emission intensities were normalized to the band-edge emission in order to compare the relative intensity of the deep-level emission. The as-grown pure ZnO nanowires exhibit an

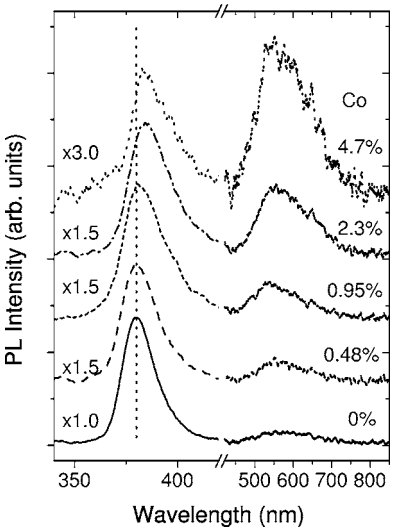

FIG. 2. Room temperature PL spectra of ZnO nanowire arrays doped with different concentration of Co. The intensities have been normalized to the band-edge emission. The vertical dotted line indicates the peak position of pure ZnO nanowires grown under similar condition. The spectra are vertically shifted and the horizontal axis has a split scale for clarity.

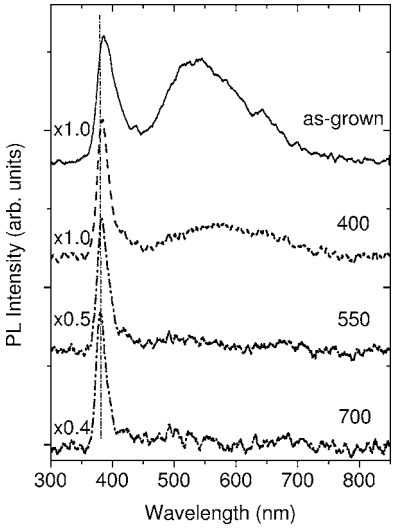

FIG. 3. Room temperature PL spectra of ZnO nanowire arrays doped with 2.3% Co after annealing at different temperatures. The spectra are vertically shifted for clarity. Annealing temperatures are labeled by the numbers above each curve. The vertical dotted line indicates the peak position of the annealed sample at 700 °C.

emission peak at 379 nm due to the near band-edge emission and a weak visible emission around 550 nm associated with the defects in ZnO.[18] As the dopant concentration increases, the peak position of the band-edge emission shifts slightly to higher wavelengths and the peak width FWHM (full width at half maximum) increases. The relative intensity of the visible emission increases significantly at higher Co concentration. In addition to the band-edge and deep-level emission, a narrow emission peak at 650 nm with increased intensity at higher Co concentration was observed. This peak may be attributed to the emission of Co^{2+} ion internal transitions in ZnO (Ref. 19) and was also observed by Lommens *et al.* in their chemically synthesized Co^{2+} doped ZnO nanocrystals.[20] The correlation of the Co^{2+} emission with magnetic properties will be discussed later.

The visible broad emission peak is commonly referred to as deep-level or trap-state emission. There are many different hypotheses on the origin of the visible emission peak, including the involvement of oxygen vacancies or interstitials,[21,22] Zn vacancies, and interstitials.[23] After a systematic study performed by Vanheusden and colleagues,[24] the deep-level peak has been attributed to the singly ionized oxygen vacancy in ZnO and the emission results from the radiative recombination of a photogenerated hole with an electron occupying the oxygen vacancy. The relative intensities of the deep-level and band-edge emission reflect the concentration of this kind of defect in ZnO. For example, the PL spectra of high-quality ZnO epitaxial thin films grown by metal organic chemical vapor deposition (MOCVD) and molecular beam epitaxy (MBE) generally have fewer defects and therefore exhibit a relatively weak deep-level emission band. In contrast, the polycrystalline thin films and powder show a strong emission band in the visible region.[18,25]

Increased concentrations of Co dopant in the ZnO nanowires simultaneously introduce additional structural and electronic defects in the material, leading to an enhancement of the deep-level emission. The Co dopant causes some distortion of the lattice (XRD results), while the spectral shape of the deep-level emission is unchanged. This suggests that the distortion results in additional oxygen vacancies in the ZnO.

The broadening of the band-edge PL emission may be explained in terms of potential fluctuations resulting from the random distribution of Co dopants in ZnO.[26–29] The microscopic inhomogeneity of the dopant concentration causes the potential fluctuation or tail states of band edges, leading to broadening of the band edge emission.

The redshift of the band-edge emission after Co incorporation may be caused by doping induced band gap renormalization effect which has been observed in Si-doped nitrides[28,30] and Ga-doped ZnO.[29] The band-gap shrinkage and free carrier screening are responsible for the band-gap renormalization effect. Recently, band-gap reduction in ZnO thin films caused by Co doping has been reported.[31–33] It was found that the band-edge emission shifted by 200–400 meV to the lower energy side when Co concentration was increased up to 15%. The band-gap shrinkage is interpreted in terms of the *s-d* and *p-d* exchange interaction between the band electrons and the localized d electrons of transition metal ions substituting Zn ions.[34–37] This interaction gives rise to a negative and a positive correction to the energy of conduction and valence bands, respectively, resulting in shrinkage of the energy gap.

Figure 3 shows the photoluminescence spectra measured on a Co-doped ZnO nanowires (sample S5A) after sequential annealing at several temperatures. While a strong deep-level emission was observed in the as-grown sample, after annealing at 400 °C, the intensity of this peak is significantly reduced. Simultaneously, the intensity of Co^{2+} emission was reduced. Annealing at 550 °C eliminates both the deep-level and Co^{2+} emission completely. In addition to the noticeable

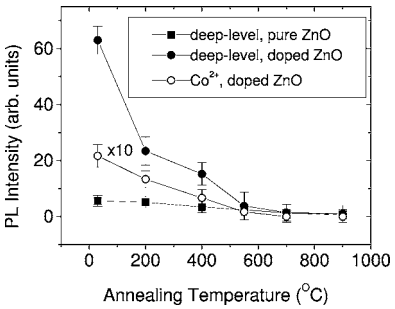

FIG. 4. Integrated PL intensity of deep-level and Co^{2+} emission as a function of annealing temperature for both Co-doped and pure ZnO nanowires.

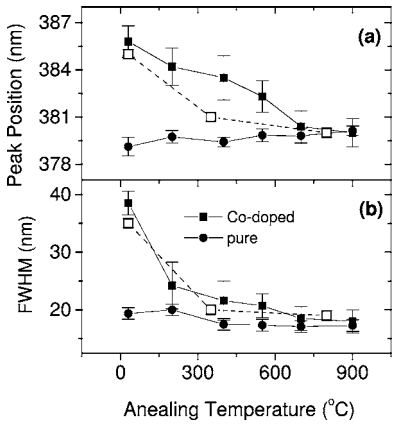

FIG. 5. PL peak position (a) and width (b) of band-edge emission as a function of annealing temperature for both pure (sample S0) and Co-doped ZnO (sample S5A) nanowires. The open squares are experimental data obtained from a similar Co-doped sample (S5B) by holding the nanowires at each annealing step for 2 h.

change in the visible regime, annealing also causes the band-edge emission to shift to a lower wavelength and the peak width to narrow.

The quantitative change in the integrated PL intensities of deep-level and Co^{2+} emission as a function of annealing temperature are plotted in Fig. 4. Experimental data from pure ZnO nanowires (sample S0) under the same annealing conditions are included for comparison. It can be seen that annealing reduces the emission intensity of the deep-level emission for both pure and doped ZnO nanowires. This indicates that annealing can effectively reduce the density of defects in the doped samples. Shishiyanu *et al.* recently reported a rapid thermal annealing of Al-doped ZnO thin films (700 nm in thickness) deposited by a chemical bath at low temperature.[38] They observed that the intensity of the deep-level emission was reduced by more than a factor of 5 after annealing at 650 °C.

As pointed out by Lommens *et al.*,[20] the peak at 650 nm is from Co^{2+} ions with strongly localized electron levels in the ZnO host. The reduction of the Co^{2+} emission as the annealing temperature is increased shows that the Co^{2+} ions in ZnO are metastable, and relax to nonradiative positions after annealing at 500 °C.

Figure 5 shows the change in peak position and width of the band-edge emission as a function of annealing temperature. The peak position shows little change while the peak width decreases slightly from 20 nm to 17.5 nm for the pure ZnO nanowires as the annealing temperature is increased up to 900 °C. In contrast, the Co-doped ZnO nanowires exhibit a large shift in peak position from 286 nm to 280 nm and a notable reduction of peak width from 39 to 20 nm after annealing at 900 °C. The reduction of the peak width may be explained by the decrease of potential fluctuations resulting from the decrease of defect density. Experimental data obtained from another Co-doped ZnO nanowires (sample S5B), which was kept at each annealing temperature for 2 h, were also included in Fig. 5 (open squares). Similar change in peak position and width were observed.

Annealing causes both the peak position and width of the band-edge emission of the Co-doped ZnO nanowires to shift to the values of the pure ZnO nanowires. This indicates that the annealing process improves the crystallinity of the doped ZnO nanowires. The small shift of the band-edge emission observed in the pure ZnO nanowires agrees with that reported on pure ZnO thin films deposited by a low-pressure MOCVD.[39] However, a much larger shift in the band-edge emission of polycrystalline thin films was reported by Cho *et al.*[40] and Chen *et al.*[41] The authors attributed their observations to quantum size effects which are associated with the crystal size in their thin films. Our samples are single crystalline nanowires with diameter of the order of 100 nm and micrometer lengths and quantum size effect should be negligible. The MOCVD-grown ZnO films are high-quality crystalline structures. Therefore, no major shift in band-edge emission was observed in these samples after annealing.[39]

In contrast to the pure ZnO nanowires, the Co-doped ZnO nanowires show a significant blueshift in the band-edge emission after annealing. This can be ascribed to the improvement of ZnO crystalline quality by annealing. The annealing at high temperature removes defects and impurities in the doped ZnO nanowires. As discussed earlier, introduction of Co impurities into ZnO causes the peak position to shift to higher wavelengths due to band-gap shrinkage as a result of the *sp-d* exchange interaction. The band-gap widening due to annealing can be viewed as the weakening of the exchange interaction due to the reduction of Co impurities in ZnO. This hypothesis is supported by XRD and TEM measurements, which suggest a precipitation of Co from ZnO crystals after annealing.

The improvement of crystalline quality as a result of annealing is also demonstrated by Raman spectroscopy and shown in Fig. 6. The as-grown sample shows a Raman peak at 437.9 cm^{-1}, which is assigned to the E_2 mode in wurtzite ZnO. The peak position for the annealed sample shifts by 1.9 cm^{-1} to a lower wave number relative to that of the as-grown sample. In addition, the annealing caused the FWHM of Raman peak to decrease from 14 to 9.7 cm^{-1}. The reduction of Raman peak width supports the improvement of the crystal quality due to annealing, consistent with the PL data. The peak position shift in the Raman spectra is likely caused by the release of compressive stress in the nanowires resulting from the removal of the defects and recrystallization of ZnO.[42,43]

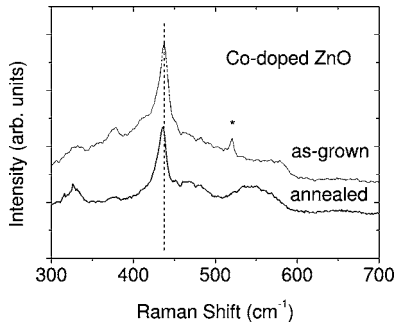

FIG. 6. Room temperature Raman spectra of as-grown and annealed Co-doped ZnO nanowires. Excitation light was an Ar ion laser at 514 nm line. The star denotes the silicon peak from the substrate.

B. Annealing effects on magnetic properties and structure

Room temperature ferromagnetism has been observed in the as-grown Co-doped ZnO nanowires.[12] Further investigations show that the ferromagnetism of Co-doped ZnO is strongly affected by an annealing process. Figure 7 shows the room temperature magnetization behavior of an as-grown sample (S5A) and those annealed at 400, 700, and 900 °C. The hysteresis loops were measured with a magnetic field perpendicular to the wire axis (i.e., parallel to the substrate surface). Note that the background signal from the substrate was subtracted from the original data. The measurements were performed on the samples after subsequent annealing steps. The as-grown sample showed a coercivity field H_C of 120 Oe and a saturation magnetization M_S of 9.5 memu. After annealing at 400 °C, the saturation was enhanced by more than 30%. Continued annealing at 700 °C causes the magnetization M_S to decrease down to 5.5 memu. The sample shows paramagnetic behavior after annealing at 900 °C.

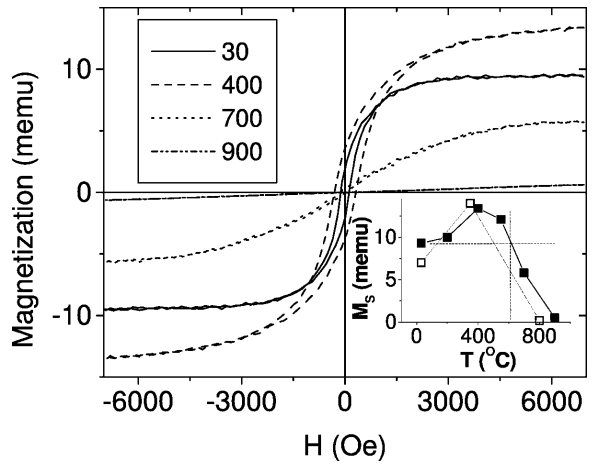

FIG. 7. Room temperature magnetization loops of as-grown Co-doped ZnO nanowires (sample S5A) and those annealed at different temperatures. The inset shows the saturation magnetization as a function of annealing temperature. The open squares show the data from a similar sample (S5B) annealed for 2 h at each step. The vertical line shows the transition temperature where the magnetization returns to the value for the as grown sample.

The inset of Fig. 7 plots the quantitative change of the saturation magnetization M_S as a function of annealing temperature. It can be seen that the ferromagnetic properties of the doped ZnO nanowires are enhanced through mild annealing (below 400 °C). Above this value, the annealing causes the magnetization M_S to decrease monotonically. The ferromagnetic properties vanish in the sample after annealing at 900 °C. The saturation M_S as a function of annealing temperature obtained from another Co-doped ZnO nanowire sample (S5B) were also shown as open squares in the inset of Fig. 7. Note that this sample was kept for 2 h at each annealing temperature for these measurements.

The effects of annealing on the magnetic properties of ZnO based DMSs were recently investigated by several research groups.[15–17] Han *et al.* found that annealing at 700 °C caused the magnetization to vanish at room temperature in their Co-doped ZnO thin films prepared at 700 °C by pulsed laser deposition.[17] They attributed the loss of ferromagnetism in the annealed sample to the reduction of charge carrier concentration in the films that in turn weakens the exchange interaction between magnetic spins. Zhang *et al.* reported that room temperature ferromagnetism could be obtained by sintering of Mn-doped ZnO bulk materials at 500 °C, but annealing the sample above 600 °C results in the decrease of magnetization, and paramagnetic properties were observed after annealing the sample at 900 °C.[16] This phenomenon was explained by the formation of a ferromagnetic metastable phase at low sintering temperature and transformation to a nonmagnetic phase at high temperature. However, Cho *et al.* observed that magnetization of CoFe codoped ZnO thin films grown at 600 °C by magnetron sputtering could be significantly enhanced by annealing the samples at 600 °C in vacuum.[15] All these studies were performed on samples grown at high temperatures, with annealing temperature above 600 °C.

Our samples, grown at low temperature, allow examination of the annealing effect up to 900 °C. The change in magnetic properties induced by annealing processes may be understood by considering both the stability of dopants and the structure of ZnO. During low-temperature annealing, the reduction of the concentration of defects as observed by PL may help reduce the disruption of the exchange interaction between magnetic spins. Another possibility is that a relaxation process takes place for the magnetic impurities, resulting in a better distribution of Co in the nanowires to reach an optimum coordination for magnetic interactions. This assumption is supported by the PL intensity reduction of Co^{2+}. By comparing our observations and the literature data (Lommens *et al.*), an anticorrelation between the Co^{2+} ions emission and ferromagnetic properties can be seen. Lommens and colleagues[20] observed a strong PL emission in their Co doped ZnO nanocrystals which exhibit a paramagnetic behavior. In our experiments, the ferromagnetic properties are enhanced and the Co^{2+} emission is diminished by a mild annealing. The samples showed a maximum magnetization at an annealing temperature around 500 °C, under which the Co^{2+} emission is also eliminated. These findings indicate that Co^{2+} ions with red emission do not contribute to magnetic coupling in ZnO. Those ions exhibiting magnetic coupling do not have a PL signature. Thus, the enhancement of ferro-

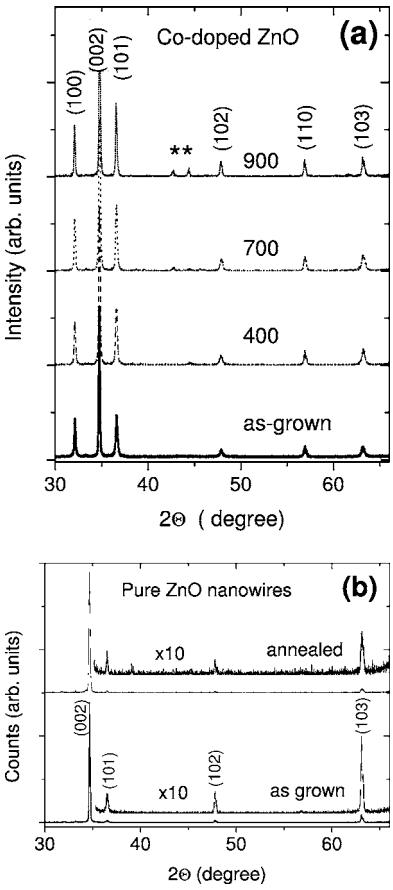

FIG. 8. (a) XRD patterns of as-grown Co-doped ZnO nanowires (sample S5A) and those after annealing at different temperatures. The stars indicate the two new diffraction peaks that evolved during the annealing process. (b) XRD patterns of as-grown pure ZnO nanowires (sample S0) and that after annealing at 900 °C. The diffraction pattern of the annealed sample is identical to that of an as-grown sample.

magnetism at low-temperature annealing may be explained by a transformation of localized electron states on Co^{2+} to those with magnetic coupling. Differential thermal analysis indicates an increase in crystalline order occurs around 260 °C, which probably represents the lowest temperature that will reduce defects and enhance ferromagnetic behavior.

The distribution of Co dopants in ZnO will be negatively affected at high temperatures. At high enough T, the thermal energy will stimulate migration of Co and result in precipitation or clustering of Co dopant. Hence, the magnetic properties may be decreased after annealing at high temperature. Evidence of Co clustering was obtained from XRD and TEM measurements on the annealed samples. Figure 8(a) shows the x-ray diffraction patterns measured on an as-grown Co-doped ZnO nanowires (sample S5A) and those annealed at 400, 700, and 900 °C. The as-grown sample shows one strong peak with index of (002) and a number of weak diffraction peaks with indexes of (100), (101), (102), (110), and (103) in the display window, indicating that the samples are aligned ZnO nanowires on the substrate. There is little change in the diffraction pattern after annealing at 400 °C. However, two new diffraction peaks around 42.5° and 44.5°

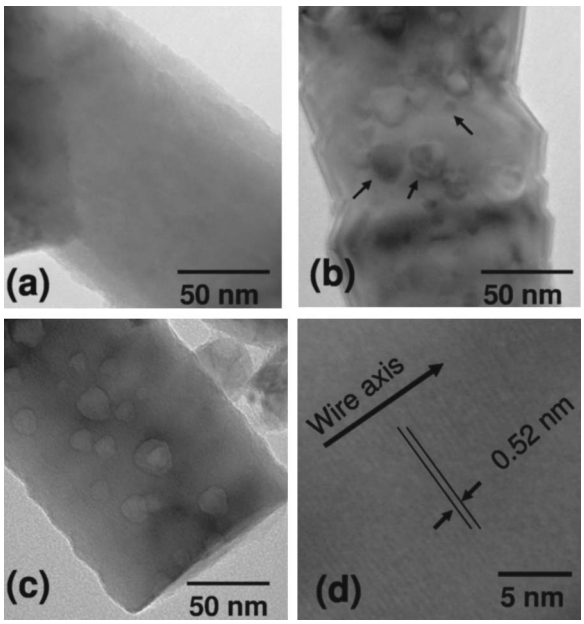

FIG. 9. TEM images of as-grown ZnO nanowires and those annealed at 900 °C. (a) As-grown Co-doped (sample S5A); (b) Co-doped nanowires (sample S5A) after annealing at 900 °C; the arrows highlight the new material phase; (c) pure ZnO nanowires (sample S0) after annealing at 900 °C; (d) high-magnification image of a regrown nanocrystal observed on the annealed Co-doped nanowire surface (sample S5A).

were observed in the diffraction pattern after annealing at 700 °C. The intensities of the two new peaks were further increased by sample annealing at 900 °C.

For comparison, the XRD pattern of undoped ZnO nanowires (sample S0) was also measured and is shown in Fig. 8(b). The as-grown and annealed pure ZnO nanowires show identical diffraction patterns. This makes it clear that the new peaks which evolved in the doped nanowires are due to the Co dopants. The positions of the two new peaks are consistent with the presence of CoO and Co_3O_4.

TEM results (Fig. 9) also suggest that the Co atoms in ZnO nanowires migrate and form cobalt oxide clusters at high temperature. The diameter of the nanowire is observed to be about 150 nm. Compared to the as-grown Co-doped samples, small crystals with contrast similar to ZnO were observed on the annealed nanowires [see Fig. 9(b)]. In addition, other clusters with greater contrast were observed. The small crystals, but not the dark clusters, were observed on the pure ZnO nanowires after annealing under the same conditions [see Fig. 9(c)]. The lattice spacing can be directly measured from a high-magnification image of the small crystals as shown in Fig. 9(d). The small crystal has a lattice spacing of 0.52 nm along the nanowire axis, which is the same as the ZnO nanowires. This suggests that the small crystals on the nanowires are ZnO homoepitaxial layer that was formed during the annealing process at high temperature.

The dark clusters are tentatively identified as the cobalt oxide clusters. However, we were unable to obtain lattice measurements on these regions. The annealed undoped ZnO nanowire sample retains its pure wurtzite structure without

an indication of a new phase after annealing. This observation is consistent with the PL data which exhibits that the band-edge emission for the annealed Co-doped nanowires shifts blue to that of pure sample due to the loss of *sp-d* exchange interaction. The decrease in the magnetization of Co-doped ZnO nanowires that resulted from annealing above 600 °C may be explained by this phase separation of Co oxides from the ZnO matrix.

Our experimental data indicates that the magnetization of Co-doped ZnO nanowires can be enhanced by annealing at any temperature below a critical value approximately 600 °C, with a maximum magnetization between 200 and 600 °C. Above 600 °C, the annealed sample exhibits a magnetization lower than the as-grown one. Despite the differences in growth conditions, our observations may be useful in interpreting the literature data. For the experiment performed by Cho *et al.*,[15] the annealing temperature at 600 °C may still fall in the enhancement temperature regime (shown in the inset of Fig. 7) and therefore resulted in the increase of magnetization. The annealing temperatures at 700 and 900 °C performed by Han *et al.*[17] and Zhang *et al.*[16] are well away from the magnetization enhancement region. Therefore, decreases in the magnetization were observed in their experiments.

IV. SUMMARY

Thermal stability of Co-doped ZnO nanowire arrays was systematically studied in terms of their structure, optical, and magnetic properties. The Co dopant was introduced into the ZnO nanowires by electrochemical-assisted hydrothermal growth at 90 °C. A wide range of annealing temperatures was covered up to 900 °C. It was found that thermal annealing caused significant changes in both optical and magnetic properties of the Co-doped ZnO nanowires.

In addition to the common luminescence features of band-edge and deep-level emission, emission peak from Co^{2+} was observed in the as-grown Co-doped ZnO nanowires. The annealing process causes the photoluminescence intensity of deep-level emission to decrease, indicating the removal of defects in the doped samples. The width of the near band-edge emission was found to shift to the values of pure ZnO nanowires, which suggests the improvement of crystal quality. The Co^{2+} ions emission was also reduced after low-temperature annealing, while the ferromagnetic properties were enhanced, with a maximum enhancement around 400 °C. Our experimental data strongly suggests that there are two kinds of sites for Co^{2+} in the as-grown samples—one contributes to paramagnetic behavior and is associated with red PL emission while the other forms ferromagnetic coupling without emission. Annealing at low temperature causes a structural relaxation and an optimized coordination of dopant ions within the ZnO matrix, resulting in the enhancement of ferromagnetic properties, likely mediated by the formation of a *d* band. Higher temperature annealing resulted in the decrease of magnetization, and paramagnetic properties were observed at room temperature after annealing at 900 °C. Along with the disappearance of ferromagnetic properties, different material phases were observed in the annealed sample. These phases were found to be the clusters of cobalt oxides that precipitated from the ZnO matrix. These cobalt oxide precipitates are likely responsible for the change in magnetic properties due to high-annealing temperature, although a reduction of the carrier concentration cannot be excluded in this study.

ACKNOWLEDGMENTS

The authors would like to thank Dr. C. Daghlian for his help with TEM measurements and Dr. Q. Zeng for his contribution to the differential thermal analysis test. This work was supported by NIST grant with Contract No. 60NANB2D0120.

[1] H. Ohno, Science **281**, 951 (1998).
[2] T. Deitl, H. Ohno, F. Matsukura, J. Cibert, and D. Ferrand, Science **287**, 1019 (2000).
[3] K. Sato and H. Katayama-Yoshida, Jpn. J. Appl. Phys., Part 2 **39**, L555 (2000); K. Sato and H. Katayama-Yoshida, *ibid.* **40**, L334 (2001).
[4] P. D. Yang, H. Q. Yan, S. Mao, R. Russo, J. Johnson, R. Saykally, N. Morris, J. Pham, R. R. He, and H. J. Choi, Adv. Funct. Mater. **12**, 323 (2002).
[5] K. Ueda, H. Tabata, and T. Kawai, Appl. Phys. Lett. **79**, 988 (2001).
[6] H. T. Lin, T. S. Chin, J. C. Shih, S. H. Lin, T. M. Hong, R. T. Huang, F. R. Chen, and J. J. Kai, Appl. Phys. Lett. **85**, 621 (2004).
[7] L. Yan, C. K. Ong, and X. S. Rao, J. Appl. Phys. **96**, 508 (2004).
[8] S. Ramanchandran, A. Tiwari, and J. Narayan, Appl. Phys. Lett. **84**, 5255 (2003).
[9] K. Rode, A. Anane, R. Mattana, J.-P. Contour, O. Durand, and R. LeBourgeois, J. Appl. Phys. **93**, 7676 (2003).
[10] Z. G. Yin, N. F. Chen, C. L. Chai, and F. Yang, J. Appl. Phys. **96**, 5093 (2004).
[11] Y. Q. Chang, D. B. Wang, X. H. Luo, X. Y. Xu, X. H. Chen, L. Li, C. P. Chen, R. M. Wang, J. Xu, and D. P. Yu, Appl. Phys. Lett. **83**, 4020 (2003).
[12] J. B. Cui and U. J. Gibson, Appl. Phys. Lett. **87**, 133108 (2005).
[13] J. J. Wu, S. C. Liu, and M. H. Yang, Appl. Phys. Lett. **85**, 1027 (2004).
[14] K. Ip, R. M. Frazier, Y. W. Heo, D. P. Norton, C. R. Abernathy, S. J. Pearton, J. Kelly, R. Rairigh, A. F. Hebard, J. M. Zavada, and R. G. Wilson, J. Vac. Sci. Technol. B **21**, 1476 (2003).
[15] Y. M. Cho, W. K. Choo, H. Kim, D. Kim, and T. E. Ihm, Appl. Phys. Lett. **80**, 3358 (2002).
[16] J. Zhang, R. Skomski, and D. J. Sellmyer, J. Appl. Phys. **97**, 10D303–1 (2005).
[17] X. H. Han, G. Z. Wang, J. S. Jie, X. L. Zhu, and J. G. Hou, Thin Solid Films **491**, 249 (2005).

[18] S. Bethke, H. Pan, and B. W. Wesseis, Appl. Phys. Lett. **52**, 138 (1988).
[19] H.-J. Schulz and M. Thiede, Phys. Rev. B **35**, 18 (1987).
[20] P. Lommens, P. F. Smet, C. M. Donega, A. Meijerink, L. Piraux, S. Michotte, S. Matefi-Tempfli, D. Poelman, and Z. Hens, J. Lumin. **118**, 245 (1996).
[21] F. A. Kroeger and H. J. Vink, J. Chem. Phys. **22**, 250 (1954).
[22] M. Liu, A. H. Kitai, and P. Mascher, J. Lumin. **54**, 35 (1992).
[23] E. G. Bylander, J. Appl. Phys. **49**, 1188 (1978).
[24] K. Vanheusden, W. L. Warren, C. H. Seager, D. R. Tallant, J. A. Voigt, and B. E. Gnade, J. Appl. Phys. **79**, 7983 (1996).
[25] Y. Chen, D. M. Bagnall, H. J. Koh, K. T. Park, K. Hiraga, Z. Zhu, and T. Yao, J. Appl. Phys. **84**, 3912 (1998).
[26] E. F. Schubert, I. D. Goepfert, W. Grieshaber, and J. M. Redwing, Appl. Phys. Lett. **71**, 921 (1997).
[27] T. Makino, Y. Segawa, S. Yoshida, A. Tsukazaki, A. Ohtomo, and M. Kawaski, Appl. Phys. Lett. **85**, 759 (2004).
[28] I. Lee, J. J. Lee, P. Kung, F. J. Sanchez, and M. Razeghi, Appl. Phys. Lett. **74**, 102 (1999).
[29] J. D. Ye, S. L. Gu, S. M. Zhu, S. M. Liu, Y. D. Zheng, R. Zhang, Y. Shi, H. Q. Yu, and Y. D. Ye, J. Cryst. Growth **283**, 279 (2005).
[30] K. B. Nam, M. L. Nakarmi, J. Li, J. Y. Lin, and H. X. Jiang, Appl. Phys. Lett. **83**, 2787 (2003).
[31] K. Samanta, P. Bhattacharya, and R. S. Katiyar, Appl. Phys. Lett. **87**, 101903 (2005).
[32] K. J. Kim and Y. P. Park, Appl. Phys. Lett. **81**, 1420 (2002).
[33] Z. W. Jin, T. Fukumura, K. Hasegawa, Y. Z. Yoo, K. Ando, T. Sekiguchi, P. Ahmet, T. Chikyow, T. Hasegawa, H. Koinuma, and M. Kawasaki, J. Cryst. Growth **237-239**, 548 (2002).
[34] A. Twardowski, T. Dietl, and M. Demianiuk, Solid State Commun. **48**, 845 (1983).
[35] L. A. Kolodziejski, R. L. Gunshor, R. Venkatasubramanian, T. C. Bonsett, R. Frohne, S. Datta, N. Otsuka, R. B. Bylsma, W. M. Becker, and A. V. Nurmikko, J. Vac. Sci. Technol. B **4**, 583 (1986).
[36] R. B. Bylsma, W. M. Becker, J. Kossut, U. Debska, and D. Yoder-Short, Phys. Rev. B **33**, 8207 (1986).
[37] Y. R. Lee, A. K. Ramdas, and R. L. Aggarwal, Phys. Rev. B **38**, 10600 (1988).
[38] S. T. Shishiyanu, O. I. Lupan, E. V. Monaico, V. V. Ursaki, and I. M. Tiginyanu, Thin Solid Films **488**, 15 (2005).
[39] Y. T. Zhang, G. T. Du, X. T. Yang, B. J. Zhao, Y. Ma, T. P. Yang, H. C. Ong, D. L. Liu, and S. R. Yang, Semicond. Sci. Technol. **19**, 755 (2004).
[40] S. Cho, Y. Kim, Y. Sun, G. K. L. Wong, and J. B. Kettterson, Appl. Phys. Lett. **75**, 2761 (1999).
[41] S. J. Chen, Y. C. Liu, H. Jiang, Y. M. Lu, Y. Y. Zhang, D. Z. Shen, and X. W. Fan, J. Cryst. Growth **285**, 24 (2005).
[42] S. S. Mitra, O. Brafman, W. B. Daniels, and R. K. Crawford, Phys. Rev. **186**, 942 (1969).
[43] F. Decremps, J. Pellicer-Porres, A. M. Saitta, J.-C. Chervin, and A. Polian, Phys. Rev. B **65**, 092101 (2002).